Statistical analysis of scars in stadium billiard

1998 J. Phys. A: Math. Gen. 31 483

(http://iopscience.iop.org/0305-4470/31/2/010)

J. Phys. A: Math. Gen. **31** (1998) 483–504. Printed in the UK PII: S0305-4470(98)84099-7

Statistical analysis of scars in stadium billiard

Baowen Li†‡‖ and Bambi Hu†§

† Department of Physics and Centre for Nonlinear Studies, Hong Kong Baptist University, China
‡ Center for Applied Mathematics and Theoretical Physics, University of Maribor, Krekova 2, 2000 Maribor, Slovenia
§ Department of Physics, University of Houston, Houston, TX 77204, USA

Received 12 May 1997, in final form 2 October 1997

Abstract. In this paper, by using our improved plane wave decomposition method, we study the scars in the eigenfunctions of the stadium billiard from a very low state to as high as about the 1 millionth state. In the systematic searching for scars of various types, we have used the approximate criterion based on the quantization of the classical action along the unstable periodic orbit supporting the scar. We have analysed the profile of the integrated probability density along the orbit. We found that the maximal integrated intensity of different types of scars scales in different way with the $\bar{h}$, which confirms qualitatively and quantitatively the existing theories of scars such as that of Bogomolny and Robnik.

1. Introduction

In the study of quantum chaos, energy-level statistics and wavefunction statistical properties are of great fundamental importance. They are proper measures to describe the signature of chaos in a quantum system whose classical counterpart is chaotic. After unfolding, the energy-level statistics has some universal behaviours in the semiclassical limit. It has been conjectured by Bohigas *et al* [1] that the level fluctuations only depend on general space-time symmetry, and are the same as predicted by the random matrix theory. Extensive numerical and experimental results have supported this conjecture (see, e.g. [2], although a rigorous mathematical proof of this conjecture is still missing.

However, despite the importance, the wavefunction of a quantum chaotic system has so far remained a relatively less studied area as compared with the energy spectra. A counterpart of WKB-ansatz, which is valid in the case of an integrable system, is still missing for a chaotic system. The only proven result is the so-called 'Shnirelman's theorem' [3], which deals with the phase-space measures associated to eigenstates of a classically ergodic system in the semiclassical limit. Shnirelman's theorem predicts that as the energy goes to infinity, the probability density of most eigenstates of a chaotic billiard approaches a uniform distribution. This is consistent with the prediction of Berry [4] and Voros [5]. One major surprise is the discovery of the strong enhancement of the probability density along the least unstable periodic orbits, which was first observed by McDonald and Kaufman [6], and later also by Heller [7] for stadium billiard. This kind of structure was named 'scar' by Heller.

Since its discovery, much effort has been made to understand this interesting phenomenon, and much progress has been achieved up to now. On the theoretical side,

‖ E-mail address: baowenli@hkbu.edu.hk

0305-4470/98/020483+22$19.50

Bogomolny [8] developed a semiclassical theory of scars in configuration space, and Berry [9] performed a similar analysis in phase space using the Wigner function. According to this theory, the intensity (see equation (6) for the definition) of a scar goes as $\sqrt{\hbar}$. Furthermore, based on the semiclassical evaluation of the Green function of the Schrödinger equation in terms of the classical orbit, Robnik [10] developed a theory, which suggests that although the geometrical structure of the scar can be determined by a single short periodic orbit (primary orbit), the maximal intensity of the scar is nevertheless determined by the sum of contributions from similar but longer periodic orbits, which 'live' in the homoclinic neighbourhood close to the stable and unstable manifolds of the primary orbit. The maximal intensity is independent of $\hbar$. The contribution of homoclinic orbits surrounding the primary orbit to the density of states has been studied by Ozorio de Almeida [11]. Most recently, Klakow and Smilansky [12] used a scattering quantization approach to study the scar problem. Parallel to the theoretical developments, there have also been many numerical [13–15] and experimental [16] studies.

Unfortunately, due to the limit of the numerical techniques and the computer facilities, most of the numerical studies so far are undertaken only in the very low-energy range, which is too low to verify the theoretical predictions in the very far semiclassical limit, especially for Robnik's theory.

In this paper, we propose a new numerical technique for solving the eigenvalue problem of two-dimensional stadium billiard. Since our method is based on the Heller's plane wave decomposition method (PWDM), we call it the improved PWDM. (For more details about Heller's PWDM, please see [17, 18].) By using this improved PWDM, we have been successful at going to as high as the 1 millionth state, which we believe is already very deep in the semiclassical regime for the stadium billiard. Moreover, with the help of the semiclassical criterion [8, 10], we have found many consecutive scars in several different energy ranges, which span two orders of magnitude in the wavenumber. With this collected ensemble of scars, we are able to study many properties of scars such as the scaling property of the scar intensity profiles with $\hbar$ up to the very far semiclassical limit.

This paper is organized as follows. In section 2 we discuss the improved PWDM which is used to calculate all the high-lying eigenstates discussed in this paper. The properties of different types of scars are discussed in section 3. In section 3.1, we discuss the scar type, whose maximal integrated intensity is independent of $\hbar$, which evidently supports Robnik's theory of scars; while in sections 3.2 and 3.3 we discuss the scar type, its geometrical structure can be predicted by Bogomolny's theory very well. More examples of scars and the bouncing ball states are also briefly discussed in section 4. We end our paper with discussions and concluding remarks in section 5. Part of the work in section 3.1 was reported earlier in [19].

2. The improved PWDM

As was mentioned previously, the difficulty of studying the eigenfunctions in the very far semiclassical limit lies in the numerical calculation of the eigenenergies and the corresponding eigenfunctions. The usual diagonalization method is not suitable because it calculates all the eigenvalues from the ground state up to a certain eigenenergy. Therefore, the dimension of the matrix to be diagonalized increases with the sequential number of the eigenstates. This drawback becomes the greatest obstacle if we want to go to the regime very far in the semiclassical limit. Among many other methods, Heller's PWDM is the most suitable one for the study of the high-lying eigenstates. In previous works, Li and Robnik [18] used this method to calculate the eigenstates as high as the 200 000th states in

a KAM and chaotic billiard. However, in order to go to even higher energy, this technique runs into the difficulty of spending too much CPU time on the matrix inversion. Thus, it is necessary to improve this method to allow us to go much higher in the semiclassical limit with suitable modern computer facilities. As we shall see in the following, our improved PWDM is at least five times faster than the PWDM, which makes it possible to test the semiclassical theory of scars.

To solve the Schrödinger equation with Dirichlet boundary conditions

$$\Delta\Psi + k^2\Psi = 0 \qquad \Psi = 0 \qquad \text{at the boundary} \tag{1}$$

we use the superposition of plane waves with the wavevectors of the same magnitude k but with different directions. The wavefunction we used for the odd–odd parity of the stadium billiard is

$$\Psi(x, y) = \sum_{j=1}^{N} a_j \sin(k_{jx}x)\sin(k_{jy}y) \tag{2}$$

where $k_{jx} = k\cos(\theta_j)$, $k_{jy} = k\sin(\theta_j)$, $k^2 = E$ is the eigenenergy, N is the number of plane waves, $\theta_j = 2j\pi/N$, i.e. the direction angles of the wavevectors are chosen equidistantly. The *ansatz* (2) solves the Schrödinger equation (1) inside the billiard, so that we have only to satisfy the Dirichlet boundary condition. For a given k, we set the wavefunction equal to zero at a finite number M of boundary points (primary nodes) and equal to 1 at an arbitrary chosen interior point. It is obvious that in order to avoid the underdetermined problem we should take $M \geqslant N$. This gives an inhomogeneous set of equations which can be solved by matrix inversion. Usually the matrix is very singular, thus the singular value decomposition method has to be invoked. After obtaining the coefficients a_j, we calculate the wavefunctions at other boundary points (secondary nodes). The sum of the squares of the wavefunction at all the secondary nodes (Heller called it 'tension') would ideally be zero if k^2 is an eigenvalue. In practice, it is a positive number. Therefore, the eigenvalue problem becomes the task of finding the minimum 'tension'. In practical implementation, it is better to look for the zeros of the first derivative of the tension (for convenience we denote this function with $f(k)$), since the derivative is available analytically/explicitly from (2) once the coefficients a_j have been found.

This is the main idea of Heller's method. In general, this method takes several (usually about 10, it depends on the step size) iterations to find an eigenvalue, which means that about 10 matrix inversions must be performed. This costs a lot of CPU time and turns out to be the main shortage of this method. So, the primary motivation of our new technique is to reduce the number of matrix inversions. As we shall soon see, this can be achieved without any difficulty.

Since we have already calculated the coefficients a_j, after one matrix inversion, the function $f(k)$ can be expanded into a Taylor series around k_0

$$f(k) = f(k_0) + \sum_{n=1} \frac{f^n(k_0)}{n!}(k - k_0)^n \tag{3}$$

where $f^n(k_0)$ is the nth derivative of $f(k)$ at k_0, which can be calculated analytically/explicitly very easily. Thus, our task is now to find the roots of this polynomial, which, as it is well known, uses much less CPU time than the matrix inversion. Then, the eigenvalue around k_0 is approximately equal to $k_0 + \Delta k$, where Δk is the smallest root of the polynomial (3). Our numerical experience demonstrates that with this improved method, we can get the eigenvalue with an accuracy of less than 1% of mean level spacing by just doing one matrix inversion. To get higher accuracy, we should use the new eigenvalue k and do

further matrix inversion. Then calculate the new coefficients a_j, and find out the smallest root of the new polynomial. This procedure can be continued until an expected accuracy is reached. In our numerical calculations, for almost all the cases, by performing about 2–3 matrix inversions we may get the eigenvalue with an accuracy as high as 10^{-4} of the mean level spacing. Therefore, our improved PWDM reduces the CPU time about five times or more as compared with the original Heller's PWDM. In our practical implementation, the function $f(k)$ is expanded up to the eighth–tenth order, which is already good enough to obtain the above-mentioned accuracy.

Before proceeding with any analysis of the scars, let us briefly discuss how to search and collect the scarred eigenstates systematically and extensively, because we need enough ensembles of the scarred eigenstates to make the numerical analysis significant. Therefore, our first step is to collect scars of the same type in a wide range of energy. We begin from a very low state, e.g. from the ground state. As long as we find the first scarred state, say, for example at the wavenumber k_0, then we can use the semiclassical criterion to estimate the next scar. According to the semiclassical theory [8–10], the scar will probably occur if quantized, i.e.

$$S = 2\pi\bar{h}\left(n + \frac{\alpha}{2}\right) \qquad n = 0, 1, 2, \ldots \tag{4}$$

S is the action along the periodic orbit, α the Maslov phase. Thus, we jump to the wavenumber at about $k = k_0 + \Delta k$ to calculate the eigenvalue and eigenfunction, where $\Delta k = 2\pi\bar{h}/\mathcal{L}$, $\mathcal{L}$ is the length of the periodic orbit. Usually, we need to calculate a few eigenstates around k to locate the scarred eigenstate. We continue this procedure until we collect a satisfied ensemble of scars. It is shown that, this procedure is very helpful in estimating the energy range of the scarred state at the very far semiclassical limit. For instance, from a very low scarred eigenstate at k_0 we can skip over a very large number of states to a rather high level, e.g. at $k = k_0 + m\Delta k$. m may be a very large number, e.g. about a few hundred. As we shall see later, in many cases this criterion is even accurate within one mean level spacing, namely, the scar occurs at the eigenstate whose eigenenergy is roughly equal to the predicted energy by this way.

However, it must be pointed out that the semiclassical theory equation (4) cannot predict the individual state at which the scar will occur. Instead, as mentioned before, if we have already found one scar, say at k_0, then the semiclassical theory just tells us that the eigenstates at the wavenumber of $k_0 \pm \Delta k$, will probably be scarred.

In our study we put $\bar{h} = 1$, so, the inverse of wavenumber k plays the role of $\bar{h}$, i.e. k goes to infinity indicates the semiclassical limit.

3. Statistical analysis of scars

In this section we would like to perform a quantitative analysis on the scars. As already mentioned in the previous section, in order to compile any significant statistics we need enough ensemble of scars of the same type. In searching and collecting the scarred eigenstates we use both qualitative and quantitative procedures. We start from very low state and calculate the probability density plots of the wavefunction for many consecutive eigenstates, usually in the order of 20. We judge, at first visually, whether the state is scarred or not by a certain kind of unstable periodic orbit (PO), e.g. diamond-shape PO or the horizontal PO. Generally, this procedure is quite accurate and reliable, although it is qualitative. Furthermore, in order to improve the objectiveness of the judgment, we calculate the integral intensity according to equation (6) to check which scarred eigenstate

is the favourite candidate. Relying on these two procedures we are able to select our scarred eigenstate very objectively and with high reliability. As long as the first scarred eigenstate is determined, we may use the semiclassical criterion equation (4) to chose the energy range in which the next scarred eigenstate will probably occur. Then repeat the procedure mentioned above and find out the next scarred eigenstate. In this way, we were able to select a sufficient number of scarred eigenstates from a huge number of eigenstates (about 10 000 eigenstates ranging from very low to about 1 millionth state) for our numerical analysis. The quantitative analysis is given in the following section.

3.1. Scars supported by the diamond-shape periodic orbit

In this section, we shall discuss a type of scar which demonstrates that the maximal integrated intensity never vanishes as $\overline{h}$ goes to zero. This finding is very different from the prediction of the commonly believed theory—single periodic orbit theory, but it can be explained by Robnik's theory, as we shall see later. The main results of this section were reported in [19], but more details about the wavefunction structures are given here.

With the help of the semiclassical quantization criterion equation (4) and the procedure described above, we have gathered about 100 examples of the same type of scarred eigenstates at different energy ranges, namely, k ranges from about 10 to $k \approx 1330$. Here, we select only six representatives of these scarred eigenstates from the very low to very high states. They are shown in figures 1(a)–(f). The eigenwavenumbers are given at the top of each figure. The lowest one, $k = 10.240\,95$ corresponds to about the 40th eigenstate, while the highest one $k = 1328.153\,849$, corresponds to the sequential number 250 034 for odd–odd parity, and to the index about 1001 408 when all parities are taken into account. To the best of our knowledge, this is the highest eigenstate showing a significant scar so far.

Suprising as it is, in addition to the eigenstate shown in figure 1(f), we have also collected quite a few examples of this type of scarred states in such a high energy. This implies that this type of scar survives the semiclassical limit. One may ask: does this finding contradict Shnirlman's theorem [3], which states that as the energy goes to infinity, the probability density of most eigenstates of a chaotic billiard approaches a uniform distribution? To test this, we have examined the statistics of the probability distribution function of the eigenstate, and found that it is an excellent Gaussian distribution function, although there is such a pronounced density around the unstable periodic orbit. The probability distribution function $P(\Psi)$ ($P(\Psi)\,\mathrm{d}\Psi$ is the probability of finding the wavefunction of value Ψ) as well as the cumulative distribution function $I(\Psi) = \int_{-\infty}^{\Psi} P(t)\,\mathrm{d}t$ are shown in figures 2(a) and (b), respectively. They are compared with the theoretical values of the Gaussian random model [4] which predicts

$$P(\Psi) = \frac{1}{\sqrt{2\pi}\sigma} \exp\left(-\frac{\Psi^2}{2\sigma^2}\right). \tag{5}$$

Even if we magnify the small details in the cumulative figure as shown in the boxes of figure 2(b), the discrepency with the Gaussian function is almost indistinguishable. Where $\sigma^2 = 1/\mathcal{A}$, should be equal to $\langle \Psi^2(\boldsymbol{x}) \rangle$, the average probability density inside the billiard, according to the semiclassical theory [3–5]. $\mathcal{A}$ is the area of the billiard.

In order to understand the scar properties quantitatively, we have investigated the following pronounced (excess) intensity in a thin tube along the periodic orbit (see figure 3),

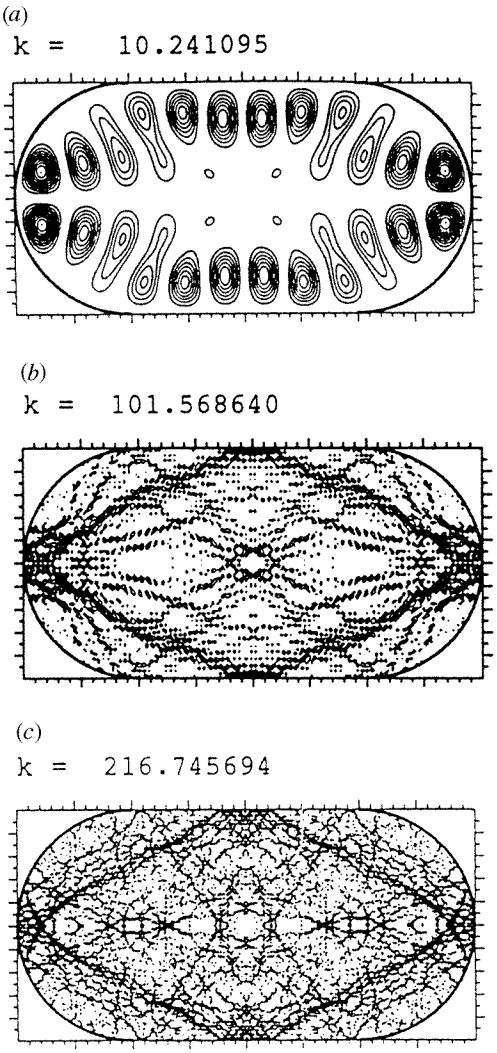

Figure 1. (*a*)–(*f*) The probability density plots of the wavefunction for six representative scarred eigenstates of odd–odd parity. The wavenumber s k are given in the figure. The highest one has $k = 1328.153\,849$, which corresponds to the index of 250 034 by using the Weyl formula (odd–odd), which corresponds to approximately the 1001 408th eigenstate for the total billiard. The scar is apparently supported by the diamond-shape periodic orbit shown in figure 3. The stadium has the parameter of circle radius $R = 1$ and the straight line length 2. In this figure, the unit length is about 211 de Broglie wavelengths.

which is defined by

$$I = \frac{\int \Psi^2(\boldsymbol{x})\,\mathrm{d}\boldsymbol{x}}{\int \langle \Psi^2(\boldsymbol{x})\rangle\,\mathrm{d}\boldsymbol{x}} - 1 \tag{6}$$

where $\Psi(\boldsymbol{x})$ is the eigenfunction at $\boldsymbol{x}$. The integral is taken over a thin tube around the periodic orbit as is shown in figure 3.

In figures 4(*a*)–(*f*), we display the integrated intensity (6) versus the width of the tube (D) in unit of the de Broglie wavelength around the periodic orbit for the scarred states

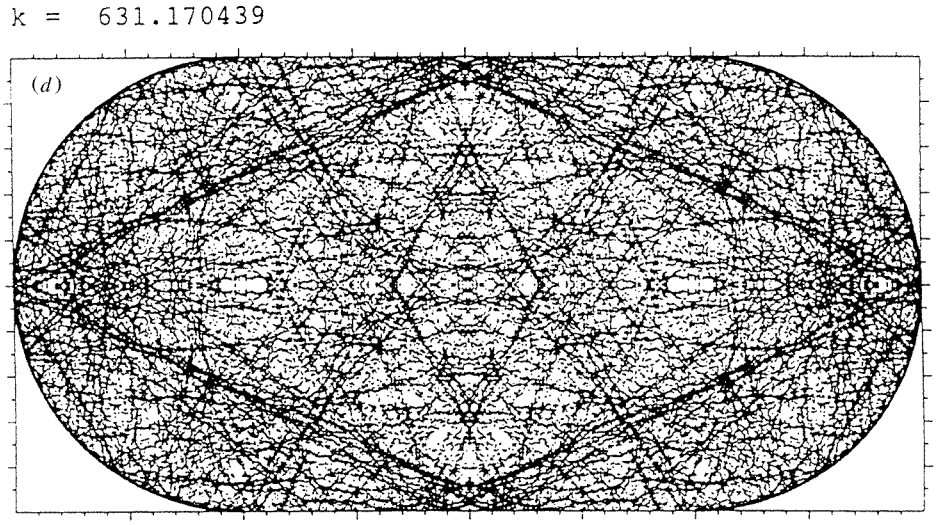

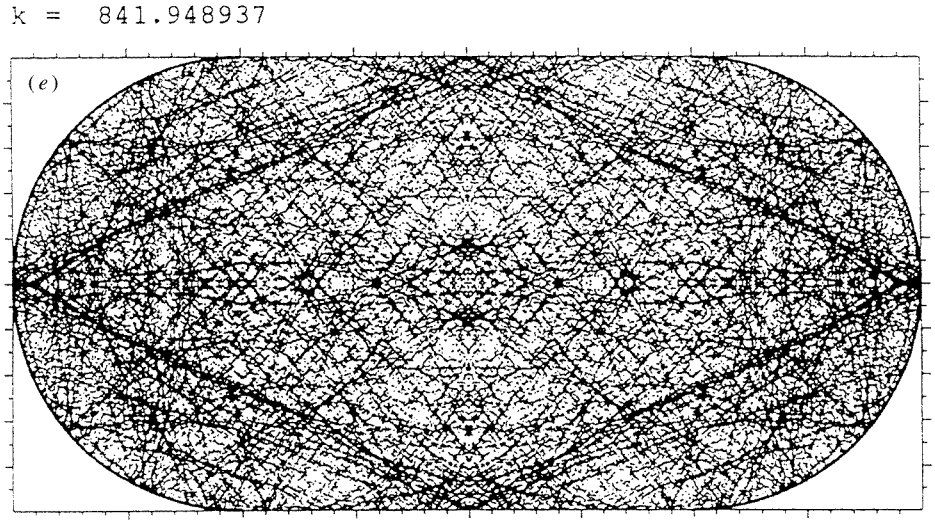

Figure 1. (Continued)

shown in figure 1. The wavenumber of each state is given at the left bottom of the box.

The first thing to be seen from these profile figures is that the scar intensity reaches a maximum at a width of about 1–2 de Broglie wavelengths from the periodic orbit. This agrees with Robnik's theory which states that the semiclassical waves associated with individual daughter orbits interfere constructively with each other only within a tube of width 1–2 de Broglie wavelengths. The second important feature of these figures is that the magnitude of the maximum does not change too much although the eigenenergy changes more than 100 times.

Furthermore, after checking the eigenenergies of these six examples carefully, we found

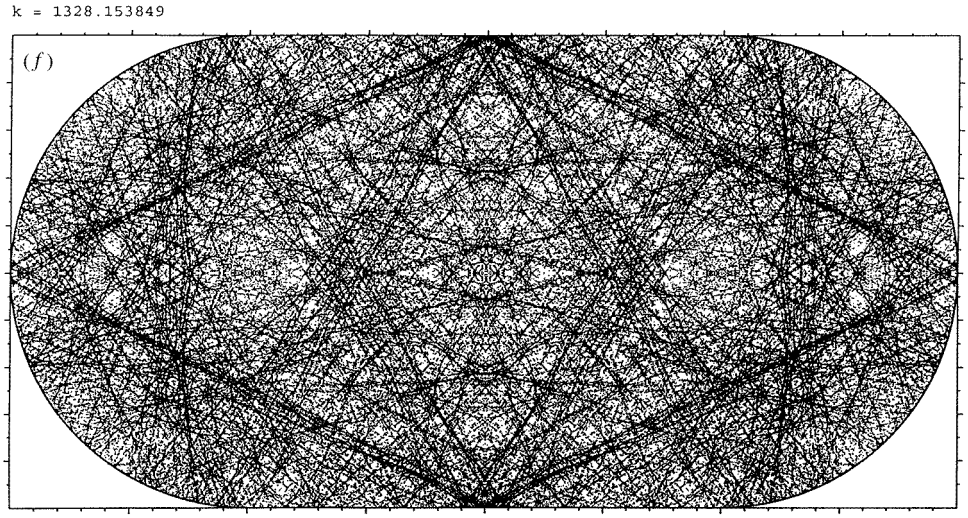

Figure 1. (Continued)

that the semiclassical criterion works very well, as mentioned in section 1, even though we go from one scarred state to another one by jumping up to a few hundred scarred states. For instance, starting from the first eigenvector $k_0 = 10.241\,095$, if we go through 65 scarred states, we have $k = k_0 + 65\Delta k = 101.563\,684$, this value is very close to the true eigenvalue $k_{\text{exact}} = 101.568\,640$. (Please note that, in this paper, we study only the eigenstates with odd–odd parity, so the length of the periodic orbit shown in figure 3 is $\mathcal{L} = 2\sqrt{5}$ rather than $4\sqrt{5}$ for the total billiard, thus, $\Delta k = 2\pi/\mathcal{L} = 1.404\,96$.) The deviation is less than one mean level spacing. This procedure also applies to many other scarred states and it can be verified readily for other states given in figure 4. The validity of the semiclassical criterion for the scarred eigenstates discussed here has also been verified very recently by Frischat and Doron [20] in studying the scars occurring in a quantum system having a mixed classical dynamics, where regular and irregular regions coexist in the classical phase space.

Now we turn to an important question, namely, the energy or $\hbar$ dependence of the maximal integrated intensity. This is a rather difficult problem, even in numerical calculations. Our numerical results show that around a certain k, the maximal integrated intensity varies from the scarred state to state. This property is clearly shown in figure 5, where we plot 26 consecutive scarred states around $k = 125$, all of these 26 eigenstates show very significant localization of the wavefunction around the periodic orbit. One interesting thing to be noted from this plot is that there are two cases, one at $k \approx 121$ and the other at $k \approx 125$ showing that two consecutive eigenstates are nearly degenerate, thus both of them are scarred. Again, from this figure we can also clearly see that the semiclassical criterion (4) works excellently, namely, the interval of the wavenumber between two scarred states is almost a constant, which is approximately equal to $2\pi/\mathcal{L}$. The maximal integrated intensity, however, fluctuates from state to state, which cannot be explained by any existing semiclassical approaches. This is still an open problem which deserves further theoretical and numerical investigations.

The results given in figure 5 imply that in order to make the study of dependence of the maximal integrated intensity on energy significant, we should take certain kinds of ensemble averaging. In our numerical study, we have performed such averaging around a certain k

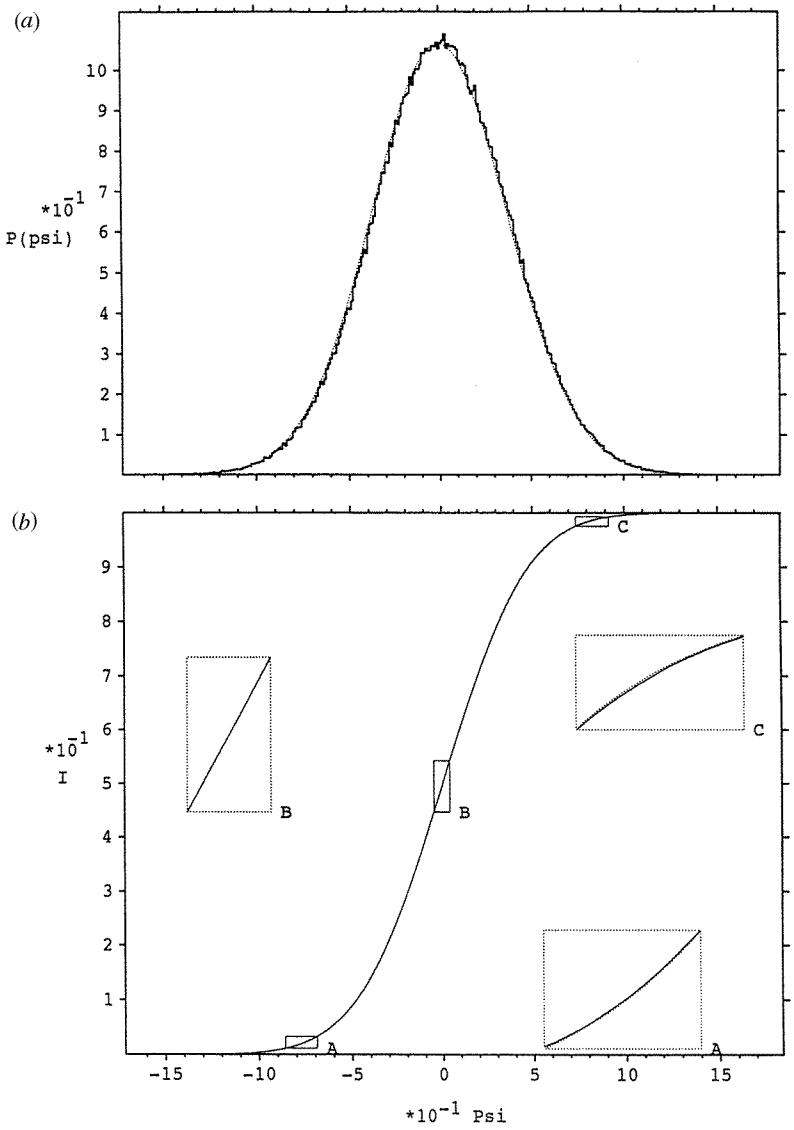

Figure 2. (*a*) The probability distribution function $P(\Psi)$ and (*b*) the cumulative distribution function $I(\Psi)$ of the eigenstate with $k = 1328.153\,849$ shown in figure 1(*f*), in comparison with the Gaussian distribution function (dotted curve). In (*b*), three small boxed regions are displayed in the corresponding magnified windows. It is readily to be seen that, even though the eigenstate is scarred, its probability distribution function is an excellent Gaussian function.

over many scarred eigenstates (usually about 10 scarred states). The averaged results are drawn in figure 6. The least-square fitting gives rise to

$$\langle I_m \rangle = 0.73/k^{\alpha} \qquad \alpha = 0.06 \pm 0.03 \tag{7}$$

where $\langle . \rangle$ is the local average over many scarred states. Obviously, the exponent $\alpha = 0.06$, which is very close to zero, is far from $\frac{1}{2}$ predicted by Bogomolny's theory. This fact indicates that the maximal integrated intensity does not depend on the energy or the $\overline{h}$ for

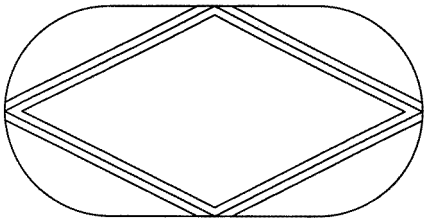

Figure 3. The integral region around the periodic orbit that is taken in equation (6). The width of the tube is D measured perpendicular to the periodic orbit.

the scar type shown and discussed in this section. This discovery is very different from the previous one [14] and cannot be explained by the semiclassical theory of Bogomolny [8] and Berry [9], however, it confirms quantitatively the theoretical prediction of Robnik [10], which states that the maximal intensity of a scar, is independent of $\hbar$, if the scar is supported by many orbits as mentioned above.

There are two important elements in Robnik's unpublished theory.

(1) The width of the scar profile is about the order of the de Broglie wavelength.

(2) There are many similar longer periodic orbits which contribute to the scar intensity.

The first one comes from a very simple physical argument. The scar profile cannot be smaller than the de Broglie wavelength since this is the smallest scale at which the quantum waves explore the classical dynamics. However, it can neither be much larger than that scale, simply because the contribution of the geometrically similar but longer periodic orbits would destroy the scar beyond the distance of one de Broglie wavelength, as the waves would interfere destructively there, while they would interfere constructively within the region of order of one de Broglie wavelength. As to the second point, the reason is that the periodic orbits, close to the stable and unstable manifolds and in the vicinity of the primary periodic orbit, complete at first a few quasicycles which are very close to the primary orbit, and only then diverge away before the final and ultimate closure. So, the first few approximate cycles of such longer orbits do resemble the primary periodic orbit, but they do not close exactly. The excursion of such orbits away from the primary orbit implies for the semiclassical waves an unavoidable loss of phase coherence beyond the distance of the order of one de Broglie wavelength away from the maximum of the scar. Taking into account all these orbits, the pronounced intensity of the scar defined by equation (6) can be described by the following formula,

$$I \approx \nu \sum_{n=1}^{\infty} \frac{\sin(nS_1/\hbar)}{\sinh(n\lambda\tau/2)} - 1 \tag{8}$$

where S_1 is the action along the primary periodic orbit, λ is the Lyapunov exponent of the primary orbit with the period of τ, the summation over n is due to the repetitions of the orbit and ν is the number of contribution orbits, which is determined by the criteria of correct phasing. Equation (8) informs us that *the maximal intensity* of the scar, when supported by many periodic orbits, is independent of $\hbar$. Finally, we would like to point out another important factor of Robnik's theory, i.e. in deriving equation (8), the averages have been taken over only one mean level spacing. Therefore, equation (8) generally applies to the individual eigenstates. This is different from the theory of Bogomolny which we shall discuss later.

Our numerical results presented in this section provide the first and very significant evidence supporting Robnik's theory. In the next section we shall discuss another type of scars which display a very different behaviour.

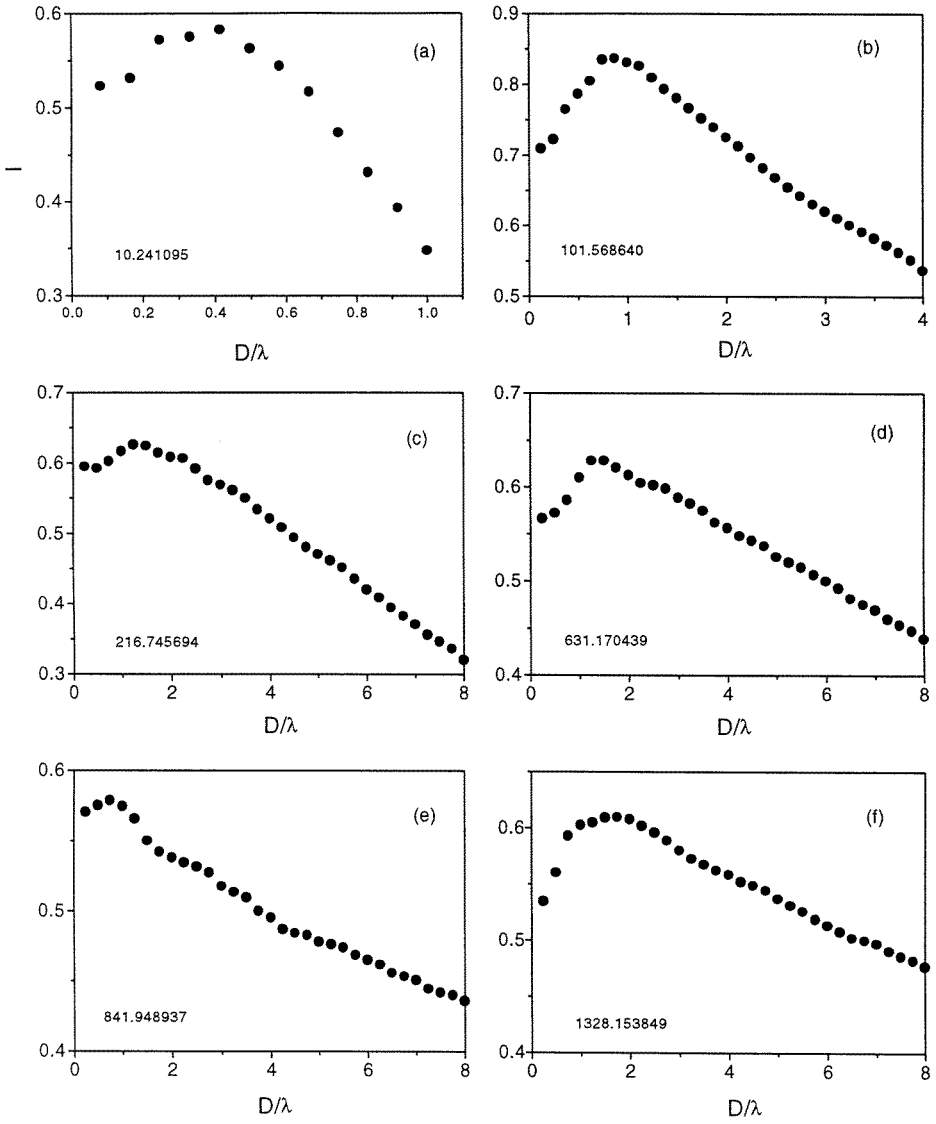

Figure 4. The integrated scar intensity profile I versus the width of the integrating tube in unit of the de Broglie wavelength for the scarred eigenstates given in figure 1. The wavenumbers are shown at the left bottom of each figure. It is very obvious that although the eigenvector varies more than 100 times, the maximal integrated scar intensity does not change too much. In fact, it is marginally a constant which is about 0.6.

3.2. Scars supported by the V-shape periodic orbit

The theoretical prediction from Robnik is different from that of Bogomolny. We should say that, however, it does not contradict that of Bogomolny at all. Instead, it is an extension of Bogomolny's theory to the scars supporting many periodic orbits. These two theories describe different types of scars. In fact, there have already been some numerical results supporting Bogomolny's theoretical prediction [14], although these numerical calculations

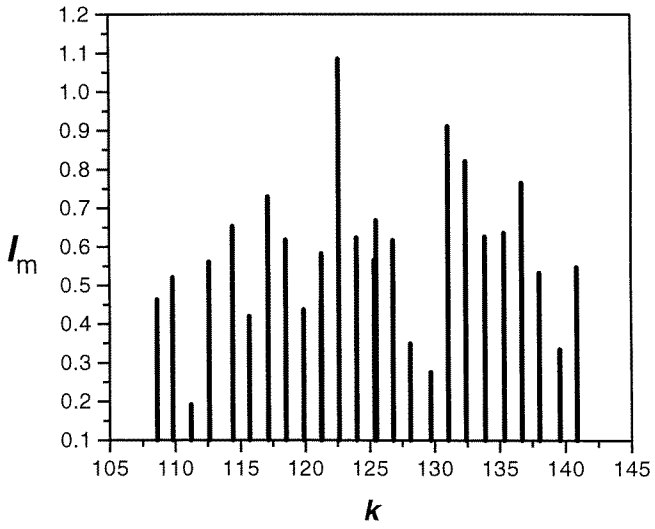

Figure 5. The maximum of integrated scar intensity versus the wavenumber k around $k = 125$ for 24 consecutive scarred states. The type of scar is the same as shown in figure 1, i.e. the diamond-shape scar. It should be noted that the interval of the wavenumber between two consecutive scarred states is very close to $2\pi/\mathcal{L}$ ($= 1.404\,96$), as predicted by the semiclassical quantization condition equation (4).

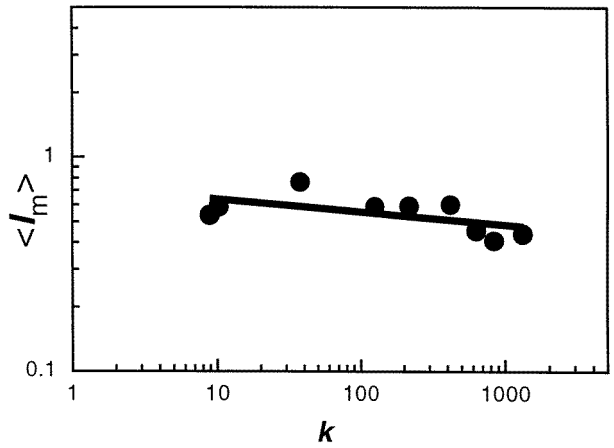

Figure 6. The locally averaged (over a small group of consecutive scarred states) maximum of the integrated scar intensity versus the wavenumber k. The full circle represents the numerical data, and the full curve is the least-square fitting, which is $0.73/k^{\alpha}$, $\alpha = 0.06 \pm 0.03$. α is very close to zero means that this type of scar survives the semiclassical limit.

are limited to very low states.

By employing our improved PWDM, we are able to go much higher than before and to test Bogomolny's theory. In our numerical investigation, in addition to the scars discussed in previous section, we have also obtained other types of scars whose maximal intensity scales with $\overline{h}$ in a very different way from that one given in (7) and (8).

Using the same strategy, i.e. the semiclassical quantization criterion, we have collected several scars of the same type. One representative in the far semiclassical limit is shown

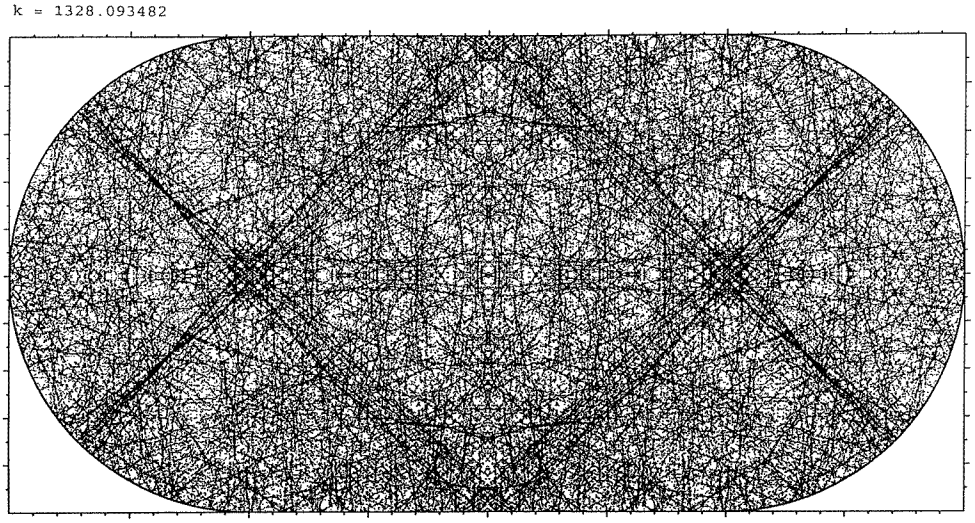

Figure 7. The probability density plot for a scarred egienstate with wavenumber $k = 1328.093\,482$, which corresponds to index 250 012 (odd–odd), and to the index about 1001 317 for the total billiard. The scar is obviously supported by the V-shape periodic orbit. There is a clear so-called self-focal point at about $x' \approx 1.85$. x' is measured from the centre of the straight line segment at the billiard boundary. This agrees very well with Bogomolny's theoretical prediction (for more details see text).

in figure 7. The scar is obviously supported by the V-shape unstable periodic orbit. (This type of scar was also observed by Heller [7] at the very low state.) The wavenumber of the eigenstate in figure 7 is $k = 1328.093\,482$, which corresponds to the index 250 012 (odd–odd), and to the index about 1001 310 for the total billiard. Again, to test Shnirelman's theorem, we have calculated the probability distribution function, this is shown in figure 8. As in the case of figure 2, the probability distribution function is a perfect Gaussian function. The integrated intensity profile is shown in figure 9. The maximal intensity is just about 0.4 which is obviously smaller than that of scar type given in section 3.1.

To look into the $\bar{h}$ dependence of such a type of scar, we have made the local averaging over a few consecutive scarred stated around a certain wavenumber k, and k changes from about 10 to about 1300. The results are given in figure 10. The least-square fitting result is

$$\langle I_m \rangle = 1.85/k^{\alpha} \qquad \alpha = 0.24 \pm 0.06. \tag{9}$$

α differs significantly from zero, thus this type of scar cannot be described by Robnik's theory. Moreover, it is not difficult to see that this type of scar has some structures. In particular, there exists points at which the wavefunction intensity is very high. To understand these properties, we shall invoke Bogomolny's theory. Accordingly, the semiclassical expression for the wavefunction is given by [8]:

$$\langle |\Psi(x', y')|^2 \rangle = \rho_0 + \bar{h}^{1/2} \sum_p \mathrm{Im} \left[A_p(x') \exp\left(\mathrm{i}\frac{S_p}{\bar{h}} + \mathrm{i}\frac{W_p^{km}(x')}{2\bar{h}} y'_k y'_m \right) \right] \tag{10}$$

the averaging $\langle \cdot \rangle$ is taken over many consecutive eigenstates (including those unscarred states). For each periodic trajectory the x'-axis is chosen along the trajectory and the y'_m axes are chosen perpendicularly to it. $S_p = \oint p_n \, \mathrm{d}q_n$ is a classical action calculated along the trajectory. $A_p(x')$ and $W_p^{km}(x')$ are classical quantities through the elements of the

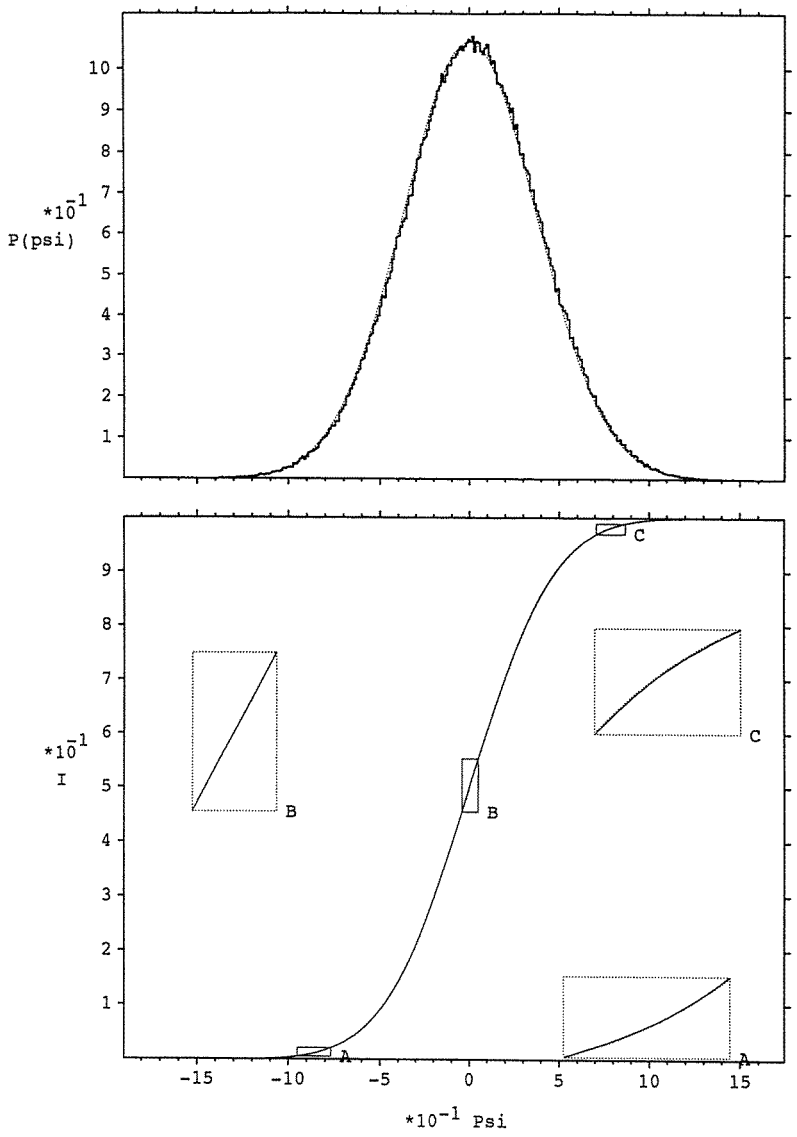

Figure 8. The same as in figure 2 but for the scarred state shown in figure 7.

monodromy matrix of a given trajectory. (The monodromy matrix of some shortest periodic orbits are given in [8].) Several conclusions can be drawn from this formula: (a) the scar has finite width perpendicular to the trajectories. It is proportional to $[\overline{h}/|W(x')|]^{1/2}$; (b) the scar strength scales as $\overline{h}^{1/2}$, which means that the scar should vanish in the semiclassical limit as $\overline{h} \to 0$; (c) there are the so-called self-focal points where the monodromy matrix element vanishes, i.e. $m_{12} = 0$.

As to the V-shape periodic orbit supporting the scar in figure 7, the self-focal points take place at the position $x' = \sqrt{L(L-R)}$, where R is the radius of the half-circle of the stadium, L the half-length of the periodic orbit. For the stadium we studied, $R = 1$ and for the V-shape periodic orbit, $L = (1+\sqrt{2})R \approx 2.414$, thus $x' \approx 1.85$. Here, x' measures

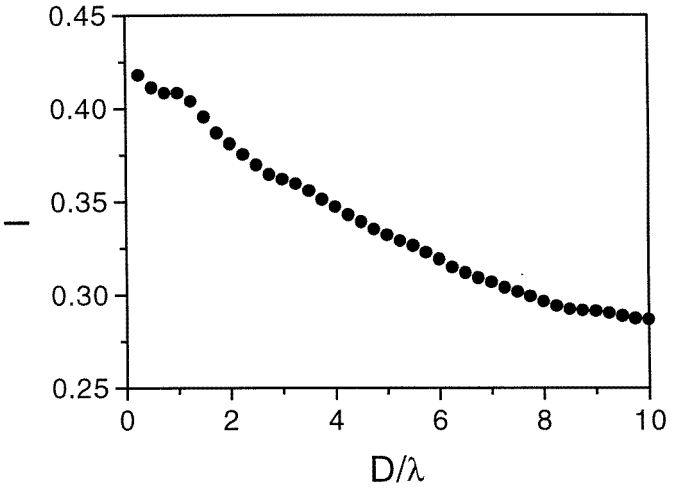

Figure 9. The integrated scar intensity profile I versus the width of the integrating tube in units of the de Broglie wavelength for the eigenstate drawn in figure 7.

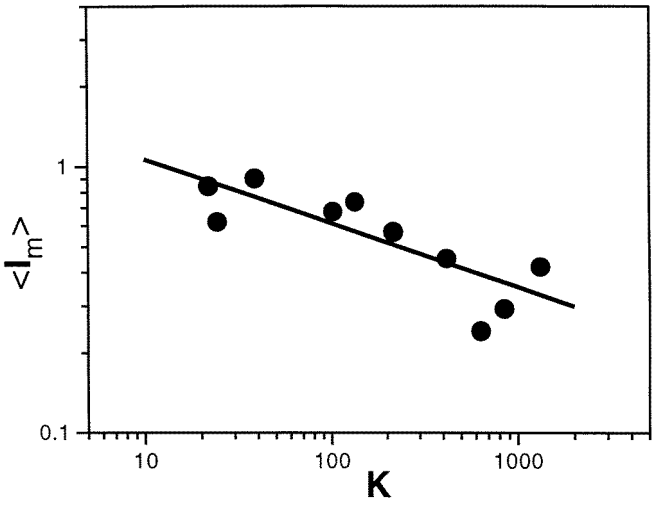

Figure 10. The locally averaged (over a small group of consecutive scarred states) maximum of integrated scar intensity versus wavenumber k. The full circles represent the numerical data, and the full curve is the least-square fitting, which is $1.85/k^{\alpha}, \alpha = 0.24 \pm 0.06$. α differs from zero significantly, which indicates that this type of scar cannot survive the semiclassical limit. It will vanish eventually if we go even deeper into the semiclassical regime.

the distance from the centre of the periodic orbit, i.e. from the centre of the straight line segment of the billiard boundary. If we take a look at the wavefunction shown in figure 7, we find out that there DO exist focal points locating at about this distance on the periodic orbit. At that point the amplitude of the probability density of wavefunction is very high. We believe that this is a very good example supporting conclusion (c) of Bogomolny's theory. Of course, this is not an accident example coinciding with Bogomolny's theory. We have more examples exhibiting this structure.

3.3. Scars supported by the horizontal periodic orbit

As further evidence, in figures 11(*a*)–(*h*) we present eight examples of scarred states for stadium with $R = 1$, $\epsilon = 0.2$, where ϵ is the half-length of straight line of the billiard. The scar in these eight states is supported by the horizontal unstable periodic orbit. It is very easy to see that the scar-shape is very similar to that predicted by Bogomolny [8] (cf figure 5 of his paper).

As a quantitative comparison with Bogomolny's theory, we shall first focus our attention on the position of the self-focal points in these scarred eigenstates. Roughly the self-focal point situates at $x' \approx 0.5$–0.6. According to Bogomolny's theory, the monodromy matrix element $m_{12} = -\frac{2}{R}(L(L-R)-(x')^2)$. In this case $L = \epsilon + R = 1.2$, so that theoretically the self-focal point should locate at $x' = \sqrt{L(L-R)} = \sqrt{0.24} \approx 0.5$, which is approximately the case in the wavefunctions shown in figures 11(*a*)–(*h*).

Furthermore, Bogomolny's theory predicts that the width of the scar shrinks with $(\overline{h}/|W(x')|)^{1/2}$, where $W(x')$ is

$$W(x') = \frac{2(L-R)}{L(L-R)-(x')^2} \tag{11}$$

for the horizontal periodic orbit. Since $L = 1.2$ and $\overline{h} \sim 1/k$, the width of the scar D is thus proportional to

$$D(x') = \frac{C}{\sqrt{k}}\sqrt{|0.24 - x'^2|}. \tag{12}$$

Now, we would like to make a quantitative comparison using this formula (12). In the following calculation, the constant C in equation (12) is determined by adjusting the width of D which is approximately equal to the scar's width at the lowest scarred state, i.e. $k = 11.994\,542$. Accidently, the choice of $C = (11.994\,542)^{1/2}$ gives us qualitatively the best result. The scar width $D(x')$ for different k is then calculated by equation (12). They are plotted in figures 12(*a*)–(*h*) corresponding to the eigenvectors k of the eigenstates in figures 11(*a*)–(*h*). Looking at these two sets of pictures, we would say that the shape, the self-focal point and also the width of the scars follow the theoretical prediction very well. Obviously, the higher the eigenstate, the better the agreement between Bogomolny's theory and our numerical results. This, of course, must be the case, because Bogomolny's theory is a semiclassical one.

Having investigated the above examples, we arrive at the following conclusion: the Bogomolny's theory determines not only the geometry of the scars, but also the intensity profile scaling with $\overline{h}$. Finally, it should be pointed out that, strictly speaking, Bogomolny's theory is based on averaging over many consecutive states (see equation (10)), however, our numerical results show that Bogomolny's function captures the main structure of the individual scarred eigenstates (see also [17]).

4. Further examples of scars and bouncing ball states

In addition to the scars illustrated in the previous section, we have also discovered quite a lot of scars, supported by other unstable periodic orbits, at about the 1 millionth eigenstate. However, because of lacking sufficient ensembles, we were not able to perform the scaling analysis as we have done in the previous section. We just show two examples here. The corresponding wavenumbers are $k = 1328.069\,060$ and $k = 1328.112\,133$, respectively. The sequential numbers are about 1000 004 and 1000 080, respectively, for the total billiard. Evidently, the scar strength is weaker than that one shown in section 3.1. It seems that these

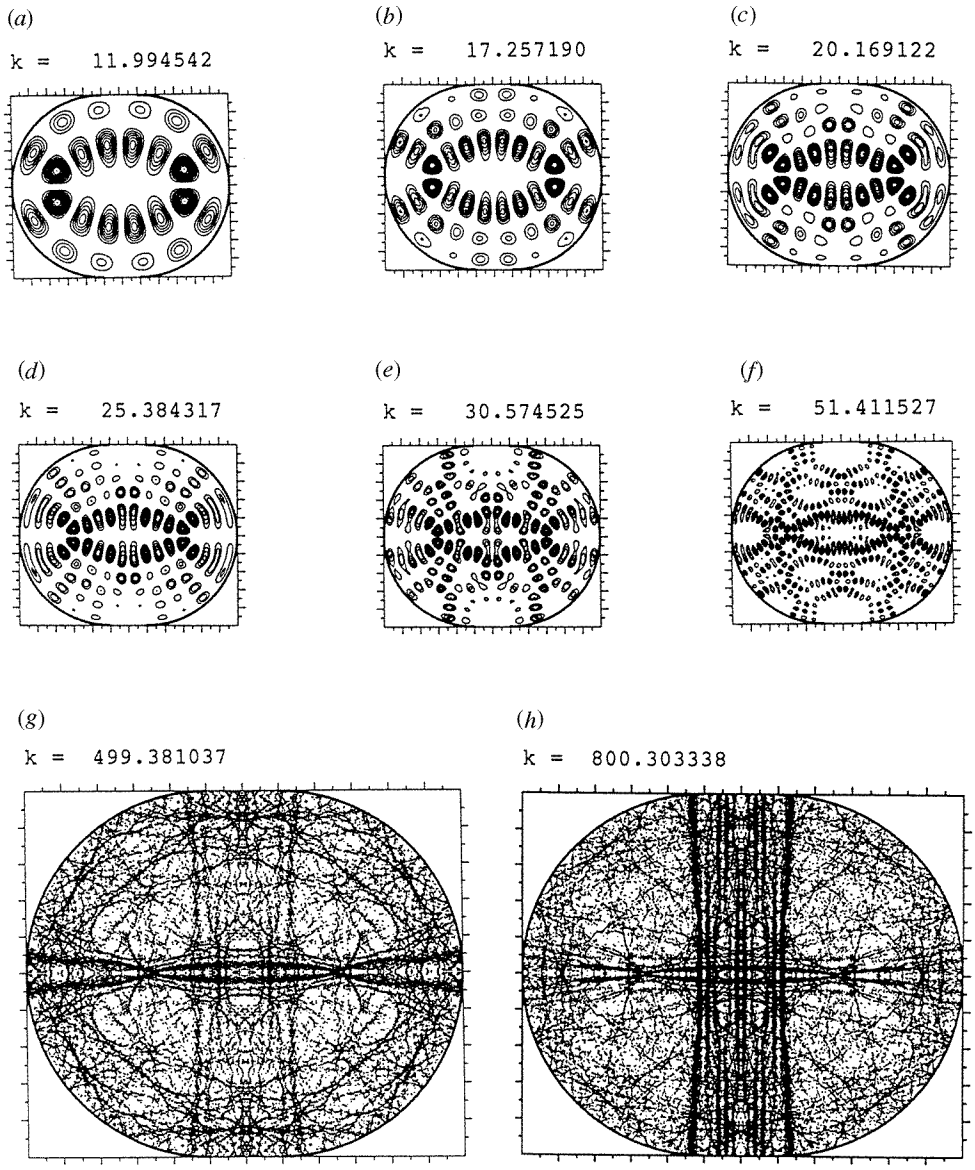

Figure 11. (*a*)–(*h*) The probability density plots of wavefunctions for eight representative scarred eigenstates (odd–odd parity) supporting by the horizontal periodic orbit. The stadium has the parameter of circle radius $R = 1$ and the straight line length 0.4. The wave numbers k are given in the figure. The highest one is $k = 800.303\,338$, which corresponds to index 49 858 using the Weyl formula (odd–odd), thus it corresponds to approximately the 200 445th eigenstate for the total billiard. The shape of the pronounced wavefunction around the periodic orbit as well as the self-focal point's position can be estimated approximately by Bogomolny's theory (see text).

scars will not be able to survive the semiclassical limit. Again, the probability distribution function $P(\Psi)$ and the cumulative distribution function $I(\Psi)$ are in good agreement with the Gaussian function as for the scarred states shown before. Thus, for most of the eigenstates,

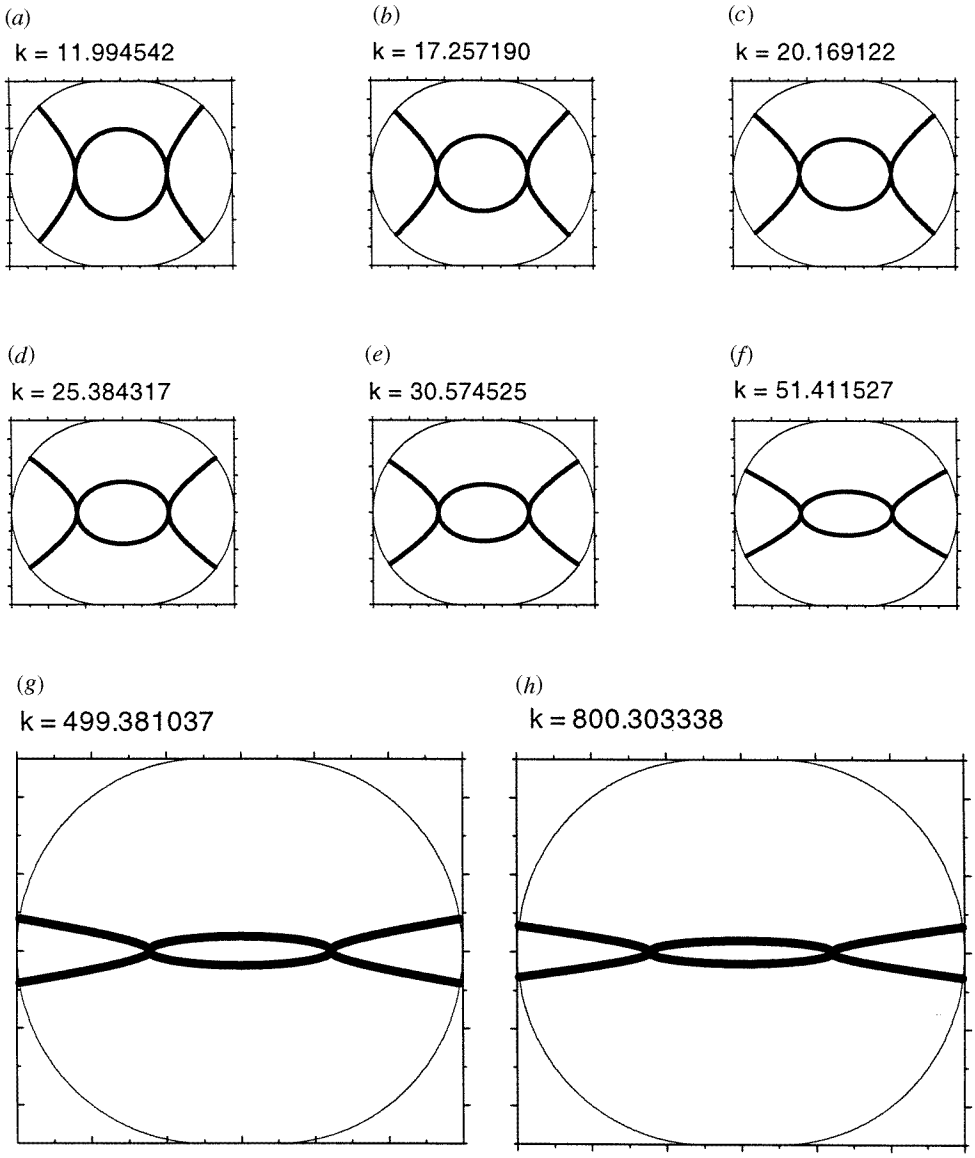

Figure 12. (*a*)–(*h*) The geometry of the scars calculated from Bogomolny's semiclassical theory. The corresponding scarred states' wave numbers are presented in the figure. The width of the scar is determined by $\frac{C}{\sqrt{k}}\sqrt{|0.24 - x'^2|}$, here the constant is so chosen that the geometry of the first one (k =11.994 542) is approximately overlap the scar's geometry shown in figure 11(*a*). Accidently, in our calculation $C = (11.994\,542)^{1/2}$. The goodness of the Bogomolny's theory is clearly seen, in particular, at the very high eigenstates such as that shown in figures 11(*g*) and (*h*). Both the self-focal point, which locates at approximately $x' \approx 0.5$, and the scar shape are roughly captured by his theory.

even though they are scarred, the Shnirelman's theorem applies in the semiclassical limit.

The bouncing ball state is a very special feature of the stadium billiard. It is well know that due to the existence of a large number of bouncing ball states, the level spacing statistics

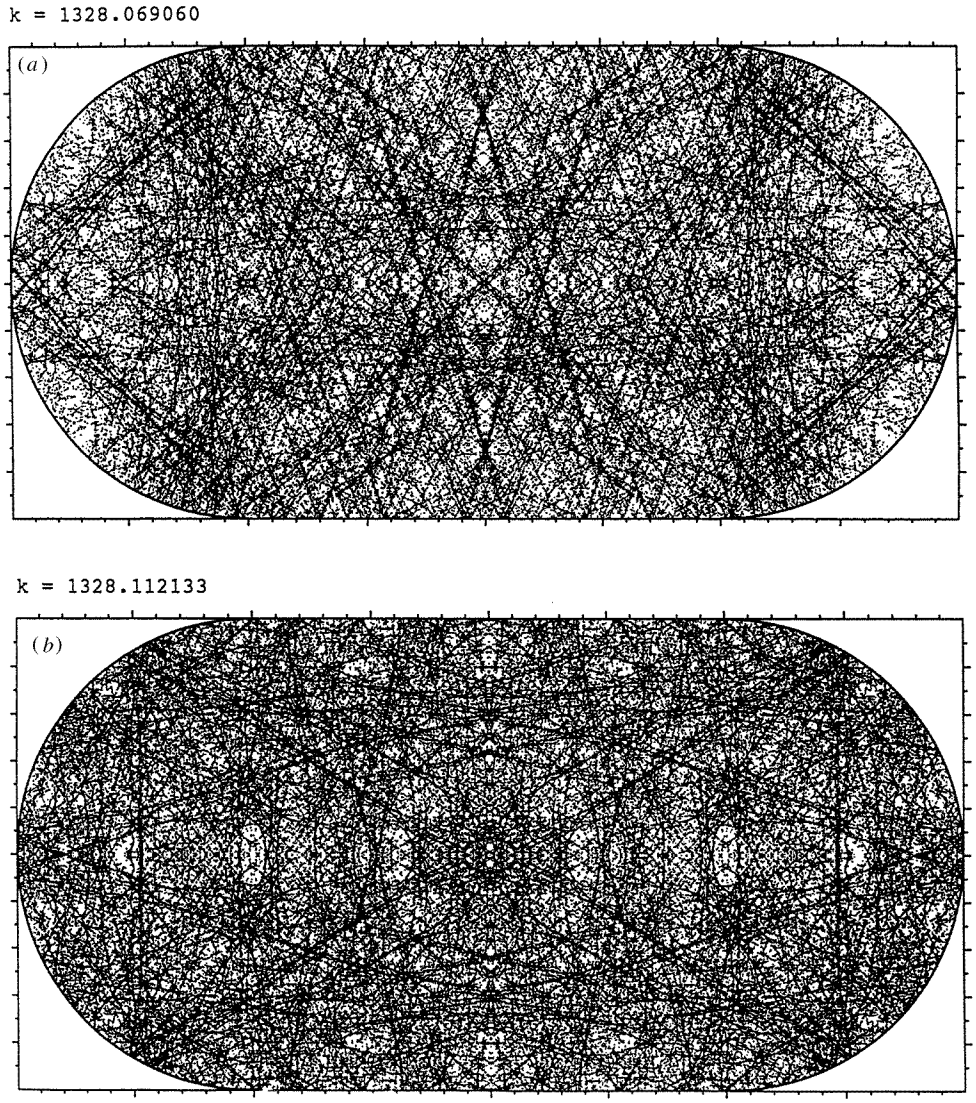

Figure 13. (*a*), (*b*) The probability density plots for two very high-lying scarred states. The scar are supported by different periodic orbits. The wave numbers are given in the figure, and the sequential number are about 250 002 and 250 019 (odd–odd), which correspond to 1001 280 and 1001 345, respectively, when all parities are taken into account.

in the stadium billiard (for $\epsilon = 1$ or larger ϵ) deviates from the GOE of random matrix theory at the lower energy range [21, 22]. We have calculated the energy level statistics by using the first 2000 levels for stadium with $\epsilon = 1$, the best-fitting gives rise to the Brody parameter $\beta = 0.83$, which is comparable with the experimental result ($\beta = 0.82$) of Gräf *et al* [21]. This number is evidently far from that value of GOE ($\beta = 1$) of random matrix theory. Therefore, as the last example of the high-lying eigenstates, we would like to show a representative of the bouncing ball states.

The bouncing ball state shown in figure 14 has an eigenvalue of $k = 1329.477\,057$. As

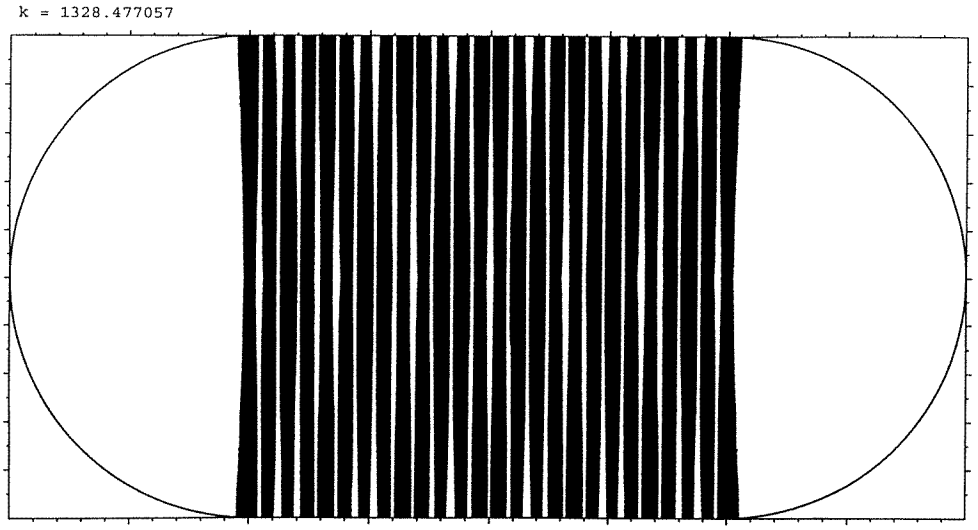

Figure 14. One representative bouncing ball state with $k = 1328.477\,057$ which corresponds to the sequential number about 250 533 (odd–odd) and 1003 405 (total billiard), respectively. Please note that the eigenvalue k is very close to the eigenvalue of a 1×1 rectangle billiard of the quantum number $m = 13$ and $n = 423$, thus $k_{nm} = 1329.521\,12$.

it should be, this energy is very close to the eigenenergy of the rectangle billiard with the side length of 1, which has quantum number $m = 13$, $n = 423$, and thus the eigenvalue $k_{mn} = 1329.521\,12$. Our numerical results demonstrate that, almost all the bouncing ball eigenstates' energy approximately obey this law. At such a high-energy level, we have observed many bouncing ball states, for instance, the three nearly degenerate consecutive states at $k = 1328.1266$, 1328.1278 and 1328.1315 showing a very distinct bouncing ball signature. For these states, the probability density distribution function deviates strongly from Gaussian.

Finally, we would like to point out that although the bouncing ball states survive the semiclassical limit, the fraction of the bouncing ball states to the total number states will nevertheless vanish in the semiclassical limit. (For more details on the fraction of the bouncing ball states, please see the two recent papers by Tanner [23] and Bäcker *et al* [24].) Therefore, the deviation of the energy-level statistics from GOE will eventually disappear in the semiclassical limit.

5. Discussions and conclusions

In this paper, we have improved Heller's PWDM, with the improved method we are able to calculate the very high-lying eigenstates, as high as about 1 millionth, of the stadium billiard with a very high accuracy (better than 10^{-4} of the mean level spacing). By using the approximate semiclassical quantization criterion equation (4), we have systematically and extensively searched and collected the scarred states in a very wide range of energies, varies from ground state to that in the very far semiclassical regime.

Our numerical results demonstrated that the semiclassical criterion (4) works very well and sometimes even accurately within one mean level spacing. Furthermore, we have analysed the scaling property of scar with $\overline{h}$. We found that the maximal integrated density

fluctuates from scarred state to state, but the locally averaged intensity scales with energy in different way for different types of scars. For the diamond-shape scar, the averaged maximal integrated density does not depend on $\overline{h}$, which implies that this type of scar survives the semiclassical limit. This finding confirms qualitatively and quantitatively Ronbik's theory of scars [10].

In addition, we have also discovered that some type of scars, for example the V-shape and horizontal bouncing ball scars, their geometrical structures such as the scar profile and the position of the self-focal point etc can be determined well by Bogomolny's theory. The width of the scar shrinks approximately with $\overline{h}^{1/2}$ for individual eigenstates as predicted by this theory, although the theory is an averaging result of many consecutive eigenstates.

Even though the eigenstates in the very high semiclassical limit are scarred, the probability distribution function is nevertheless an excellent Gaussian function, which verifies the Shnirelman's theorem.

As illustrated by the examples in this paper, the wavefunctions of eigenstates contain so rich structures that the nowadays semiclassical theory cannot predict all of them in detail. There is still a long way for us to go to be able to predict the wavefunction structures of a given individual eigenstate. But, we believe that the periodic orbits theory could contribute more in this direction.

Acknowledgments

We would like to thank the referees for helpful and stimulating suggestions and comments. BL would like to thank Professor Dr Marko Robnik for discussions. He is also very grateful to Professor Dr Felix Izrailev for helpful discussions during the STATPHYS 19 in Xiamen (1995) and during his visit to Como (1996). This work was supported in part by the Hong Kong Research Grant Council grants and the Hong Kong Baptist University FRG. The work done in Slovenia was supported by the Ministry of Science and Technology of Republic of Slovenia.

References

[1] Bohigas O, Giannoni M-J and Schmit C 1984 *Phys. Rev. Lett.* **52** 1
[2] Bohigas O 1991 *Proc. Les Houches Summer School 'Chaos and Quantum Physics' (Les Houches, Session LII)* ed M-J Giannoni, A Voros and J Zinn-Justin (Amsterdam: Elsevier)
[3] Shnirelman A L 1974 *Usp. Mat. Nauk.* **29** 181
[4] Berry M 1977 *J. Phys. A: Math. Gen.* **12** 2083
[5] Voros A 1979 *Stochastic Behavior in Classical and Quantum Hamiltonian Systems (Lecture Notes in Physics 93)* ed G Casati and J Ford (Berlin: Springer) p 326
[6] McDonald S W and Kaufman A N 1979 *Phys. Rev. Lett.* **42** 1189
McDonald S W 1983 *PhD Thesis* Lawrence Berkeley Laboratory Report No LBL-14837
[7] Heller E J 1984 *Phys. Rev. Lett.* **53** 1515
[8] Bogomolny E B 1988 *Physica* **31D** 169
[9] Berry M 1989 *Proc. R. Soc.* A **423** 219
[10] Robnik M 1989 *Preprint of ITP* University of California at Santa Barbara
[11] Ozorio de Almeida A M 1989 *Nonlinearity* **2** 519
[12] Klakow D and Smilansky U 1996 *J. Phys. A: Math. Gen.* **29** 3213
[13] Waterland R L, Yuan J-M, Martens C C, Gillilan R E and Reinhardt W P 1988 *Phys. Rev. Lett.* **61** 2733
Eckhard B, Hose G and Polak E 1989 *Phys. Rev.* A **39** 3776
[14] Wintgen D and Hönig A 1989 *Phys. Rev. Lett.* **63** 1467
Agam O and Fishman S 1994 *Phys. Rev. Lett.* **73** 806
[15] Prosen T and Robnik M 1993 *J. Phys. A: Math. Gen.* **26** 5365
[16] Sridhar S and Heller E J 1992 *Phys. Rev.* A **46** 1728

Stein J and Stöckman H-J 1992 *Phys. Rev. Lett.* **68** 2867
[17] Heller E J 1991 *Proc. Les Houches Summer School 'Chaos and Quantum Physics' (Les Houches Session LII)* ed M J Giannoni, A Voros and J Zinn-Justin (Amsterdam: Elsevier, North-Holland) p 602
[18] Li B and Robnik M 1994 *J. Phys. A: Math. Gen.* **27** 5509
Li B and Robnik M 1995 *J. Phys. A: Math. Gen.* **28** 2799
[19] Li B 1997 *Phys. Rev.* E **55** 5376
[20] Frischat S and Doron E 1997 *J. Phys. A: Math. Gen.* **30** 3613
[21] Gräf S W, Harney H L, Lengeler H, Lewenkopf C W, Rangacharyulu C, Richter A, Schardt P and Weidenmüller H A 1992 *Phys. Rev. Lett.* **69** 1296
[22] Sieber M, Smilansky U, Creagh S C and Littlejohn R G 1993 *J. Phys. A: Math. Gen.* **26** 6217
[23] Tanner G 1997 *J. Phys. A: Math. Gen.* **30** 2863
[24] Bäcker A, Schubert R and Stifter P 1997 *J. Phys. A: Math. Gen.* **30** 6783